Journal of Alloys and Compounds 489 (2010) 103–109

Contents lists available at ScienceDirect

Journal of Alloys and Compounds

journal homepage: www.elsevier.com/locate/jallcom

Evaluation of mechanical properties and structure of multilayered Al/Ni composites produced by accumulative roll bonding (ARB) process

A. Mozaffari, H. Danesh Manesh*, K. Janghorban

Dept. of Materials Science and Eng. School of Eng., Shiraz University, Shiraz, Iran

ARTICLE INFO

Article history:
Received 12 July 2009
Received in revised form 3 September 2009
Accepted 6 September 2009
Available online 11 September 2009

Keywords:
Accumulative roll bonding
Composite materials
Mechanical properties
Microstructure
Metals and alloys
Scanning electron microscopy

ABSTRACT

Multilayered Al/Ni composites were produced by accumulative roll bonding (ARB) process using Al 1060 and commercial Ni foils. In this process it was observed that nickel layers necked and fractured as accumulative roll bonding passes increased. After six ARB passes, a multilayered Al/Ni composite with homogeneously distributed fragmented nickel layers in aluminum matrix was produced. Structure and mechanical properties of these multilayer composites were evaluated at different passes of ARB process. During ARB, it was observed that as the strain increased with the number of passes, the strength, microhardness and elongation of produced composites increased as well. In addition, enhancement of the strength was shown to be higher than the tensile strength of Al/Al and Al/Cu multilayered composites produced by ARB process in the previous works by the same authors.

1. Introduction

Techniques of severe plastic deformation have been of continual interest in the production of novel metallic microstructures. Among these, accumulative roll bonding has been extensively used to produce nanocrystalline [1–10], as well as two phase nanocomposites [2,5,11–21]. Besides there are several reports of mixing and phase evolution of multicomponent systems during ARB processes [2,7,12,14,21]. In this technique, two strips of similar or dissimilar alloys are rolled together for several passes. In the simple case of two component system, the final structure consists of multilayers, which refines progressively with continuation of ARB process. The evolution of microstructures and related mechanical properties during ARB cycles at room temperature were studied for several metal strips such as commercial pure Al [1,3,4], Al based alloys [6], Cu–Ag alloys [7], Zr based alloys [8], IF steels [4,8] and multilayer strips such as Al/Ni [11,12], and Al/steel [13], Ti/Al/Nb [14], Ti/Zr/Ni [15], Ti/Ni [16,17], Al/Pt [18], Al/Hf [18], Cu/Nb [19], Fe/Ag [20], and Al/Mg [21].

Interests in ARB are focused on mechanisms of grain refinement and the effect of strain on microstructural evolution. Concurrently, the average grain size of the two components is known to refine as the layered structure refines [12,15,20]. In the limit where the layers breakdown and the alloy reach a steady state structure, it is possible to form solid solution alloys, intermetallics and nanocomposite structures, depending upon the thermodynamics of the system and the characters of the mixing process [11,14–17]. Generally, metallic multilayer composites are produced by coating processes like ion sputtering and evaporation in order to make thin films [22–24] or by diffusion bonding of thin strips of different materials. Recently, production and development of bulk multilayer composites by means of deformation processes like 'repeated press and rolling' [20,25] and 'repeated folding and rolling' [5,26] have been practiced due to economical benefits as well as capability of mass productions [27]. It should be noted that most of the deformation processes require expensive tools and complex processes which have limited use at commercial and industrial scales. However, ARB process can be used as an innovative and appropriate way of multilayer composite production for the sake of its simplicity and cheaper primary commodity. With respect to other methods, the ARB process of elemental foil arrays allows for the retention of high purity during sample preparation [2,21]. This is because, during deformation, the large interlayer interface areas are not exposed to the atmosphere. In addition, the sample temperature does not increase significantly above the ambient temperature during the process under low deformation rate (i.e., about 1 s^{-1}) [4,5].

Severe plastic deformation by ARB for similar metals and alloys causes grain refinement by formation of IDB's (incidental dislocation boundaries) and GNB's (geometrically necessary boundaries). This leads to an ultrafine grained structure and equilibrium grain boundaries [1,4,7,12]. Mostly, during co-deformation of dissimilar metal systems, plastic instabilities in one of the layers occur

* Corresponding author. Tel.: +98 9173149475 (mobile); fax: +98 7112307293.
E-mail address: daneshma@shirazu.ac.ir (H. Danesh Manesh).

0925-8388/$ – see front matter © 2009 Elsevier B.V. All rights reserved.
doi:10.1016/j.jallcom.2009.09.022

earlier than the other due to differences in mechanical properties. As strain increases, the harder layer experiences necking and premature fragmentation [2,11,12,14–21]. Multilayer foils have been of great interest owing to their new structural, chemical, magnetic, optical and electronic properties [14,19,22–24]. Especially, the Al–Ni system has been studied thoroughly as a model system for its attractive applications as coatings and microstructural features [11,12,23,28,29]. In the past studies, thin Al/Ni multilayers were mostly deposited by sputtering [23] or electron beam evaporation [28], while accumulative roll bonding process [12] and repeated folding and cold rolling of Al and Ni sheets and foils were also applied as an alternative process to produce the Al–Ni multilayer sheets and foils [5,11,29]. ARB provides a relatively inexpensive process, because starting materials are metal sheets or foils. These metal sheets and foils are available in a wide variety of thickness and purity, as compared with specially deposit layers. The ARB process also has a few problems; the most important defect of this method is edge cracks that form at the higher ARB cycles—these cracked parts should be trimmed.

In this study the Al/Ni multilayer composites were produced by ARB process. In addition to the microstructural studies mechanical properties of produced composites were investigated at different passes of ARB for the first time. Finally the properties of these composites were compared with Al/Cu multilayer composite [2] and Al nanostructure strip [3] produced previously by the same authors.

2. Experimental procedure

2.1. Materials

Aluminum 1060 and commercial nickel foils (99.6% pure) were used as primary materials. Ni foils 100 μm thick and Al foils 100 μm thick were used in this study as listed in Table 1.

2.2. Production of Al/Ni multilayer composites

Foils with dimensions of about 60 mm × 120 mm were cut from the stock sheets, and were degreased in acetone for 30 min and then were scratch brushed. 6 Ni and 5 Al foils were then stacked alternatively to produce a 1.1 mm thick multilayer sample with composition of 35%Al–65%Ni by atomic weight. This 1.1 mm thick sample was rolled down to a 0.7 mm thick sandwich. This initial sandwich was cut into equal pieces in length and then degreased, scratch brushed and stacked for ARB process.

ARB of the primary Al/Ni sandwiches involved two main steps: first the surface was degreased in acetone, air dried and then scratch brushed by a circular steel brush. The second step was concurrent rolling of the stacked sandwich samples using a 170 mm diameter roll mill at a rolling speed of 15 rpm which was repeated 6 times at room temperature and generated a 5.3 equivalent strain in the multilayer composites. Cold roll bonding was conducted under the condition that the reduction in thickness per cycle of ARB process was 50% ($\varepsilon = 0.8$/cycle), including $\varepsilon = 0.5$ for the primary sandwiches.

2.3. Evaluation of structure

Rolling cross-section of multilayer composites was prepared for evaluation of its structure by scanning electron microscope. Both unetched and etched microstructures were investigated. For metallography, samples were mounted using a conductive epoxy and then ground and polished by 1 μm diamond paste in the last polishing step. Electrical etching was performed using 5 ml HBF4 – fluoboric acid 48% – and 200 ml distilled water. Chemical compositions gradient of the interface of layers were determined by an EDX spectrometer and corrected by ZAF factor using Link ISIS software and calibrated by using pure Ni and Al standards.

2.4. X-ray diffraction analysis

The X-ray diffraction technique was used for phase identification of produced composites. Diffraction patterns were recorded using a Philips X'Pert diffractometer employing Cu K_α at room temperature. The data were collected for diffraction angles $35^O \leq 2\theta \leq 105^O$, with a step width of 0.05^O and a step time of 1 s. The diffraction was performed on the cross-sections of 10 samples.

2.5. Mechanical properties of Al/Ni multilayer composites

Tensile test was performed for composite samples by an Instron tensile machine at a strain rate of $8.3 \times 10^{-4}\ s^{-1}$ at room temperature. Tensile test samples were prepared with 8 and 3 mm in gage length and width, respectively which correspond to one fifth of the JIS-5 standard dimensions [2,3]. Vickers microhardness was measured by a Leitz apparatus under a load of 15 g and time of 15 s on composites' cross-sections perpendicular to the rolling direction. Microhardness test was carried out on both aluminum matrix and nickel layers in more than seven points and the average value was reported.

3. Results and discussion

3.1. Structure

Fig. 1 illustrates macrostructure variations of Al/Ni composites during different ARB cycles. It is evident that nickel layers were coherent just in the first cycle of sandwich production, Fig. 1a, and then they initiated to neck and fracture locally in subsequent cycles. Finally nickel layer separation was observed in the sixth cycle (Fig. 1b–d). After six cycles of ARB process, a composite with aluminum matrix and homogeneously distributed Ni fragments in the matrix were achieved (Fig. 1d). Al matrix acts as a transfer media for load to the Ni foils and fills up all spaces between the Ni layers. Fracture is ductile as shown by the elongated ends of Ni foils (Fig. 2).

Fig. 2 shows that appropriate bonding with a uniform interface is created between adjacent aluminum and nickel layers in six cycles of ARB. Corresponding to Fig. 1, as ARB process cycle increases, there is an increase of strain and also a decrease in the thickness of nickel layers. The two metals adhere rather quickly on initial rolling, and then, stress builds up and Ni layers yield, neck and fracture at several points. It was shown in Fig. 1 that nickel layers elongated during the first cycle of ARB and preserved their coherency in most of the regions. After the second cycle, necking, fracture and separation of Ni layers took place through the samples (Fig. 2). Generally, during plastic co-deformation of dissimilar metals, instabilities originate due to differences in mechanical properties of layers (Al and Ni layers) causing the advent of necking and fracture in the harder layer (Figs. 1 and 2) [2,12,14,19–21]. It should be mentioned that difference in mechanical properties of two dissimilar layers of Al/Ni composites leads to inhomogeneous fragmentation of nickel layers in the form of small parts inside the Al matrix (Fig. 1a and b). This effect becomes weaker as the number of cycles increases and mechanical properties of the matrix and reinforcements are closer resulting in a homogeneous deformation of Ni layers inside the Al matrix (Fig. 1d).

Variations of nickel layer thickness were measured and are shown in Fig. 3 versus the number of ARB cycles. It shows a rapid decrease of Ni layer thickness during the initial ARB cycles and leveling off after the second cycle which is due to fracture of the Ni layers. The deformation of the layers was followed by measuring their thickness along intercepts perpendicular to the rolling direction drawn at several random positions of the SEM micrographs; 150–200 layers were observed each time. With attention to Fig. 4, the frequency distribution of Ni layer thicknesses broadened quickly to 2nd cycle of ARB process (Fig. 4a) and became

Table 1
Specifications of Al and Ni foils.

Materials	Chemical composition (wt.%)	Sheet dimensions (L, W, t) (mm × mm × mm)	Hardness (VHN)	Elongation (%)	Yield strength (MPa)
Commercial pure aluminum foil 1060	99.5 Al, 0.20 Si, 0.25 Fe, and 0.05 Cu	120 × 60 × 0.1	27	13.2	34.7
Commercial pure nickel foil	99.6 Ni, 0.3 Mn, 0.05 Si, and 0.05 Fe	120 × 60 × 0.1	81	9.8	126.4

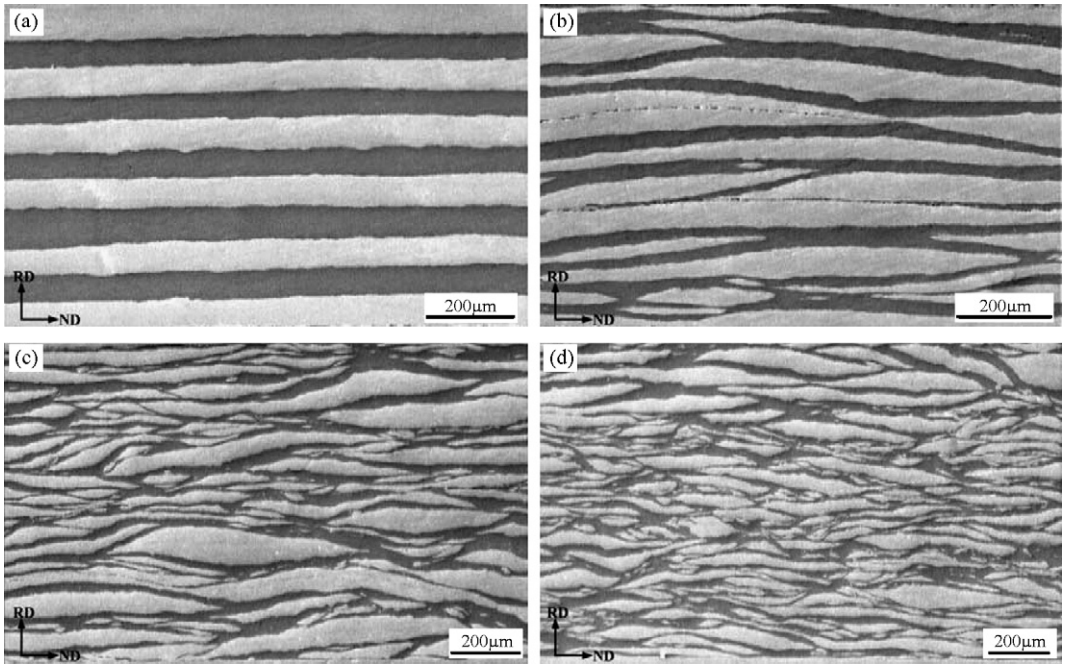

Fig. 1. SEM micrographs of the ARB processed Al/Ni multilayer composites showing cross-sections of (a) primary sandwich, (b) 2 cycles, (c) 4 cycles and (d) 6 cycles.

narrow after 6 cycles of ARB (Fig. 4c). The thickness distributions are well fitted by the log normal function in various cycles of ARB that demonstrated in Fig. 4. It should be also mentioned that ultra fine layers with thickness less than 10 μm were observed at sixth cycle of ARB in various points. This behavior was reported for other co rolled bimetallic foils too [29].

Fig. 5 shows the SEM image of nickel and aluminum layers (electro etched) after different passes of ARB process. With attention to this figure, grain refinement and elongated grain microstructure within rolling direction are created by increasing the ARB strains. Arrow A in Fig. 5c shows a shear band that divides the elongated grain of aluminum layer to subdivisions and penetrated the adjacent Ni layer too.

Min et al. [12] demonstrated that shear bands in the matrix around the interface of matrix and reinforcement move inside the hard phase due to its lower formability and cause shear and separation in hard phases as shown in Fig. 5c with arrow A. In the early stages of ARB process, the length of the Ni layers is more than the distance of shear bands, and consequently, incoherent fragmentations along the layers are created (Fig. 1b and c), but as ARB proceeds, Ni layers are traversed and shortened by shear bands, and ultimately a macrostructure with Al matrix and reinforcing Ni fragments with lengths shorter than shear band size is created in the rolling direction (Figs. 1d and 2). Considering the basics of ARB process, thickness of Ni layers decrease with increasing the number of cycles, and this leads to thicknesses far less than the original thickness. The same trend is also shown in Figs. 3 and 4. As Fig. 5 demonstrates, non-uniform structural variations – specifically in the interface of Al matrix and Ni layers – originate from inhomogeneous interaction of matrix and reinforcement layers. These are in turn due to the different flow stresses of phases, friction between Al matrix and Ni layers, and the friction between rolls and sample sur-

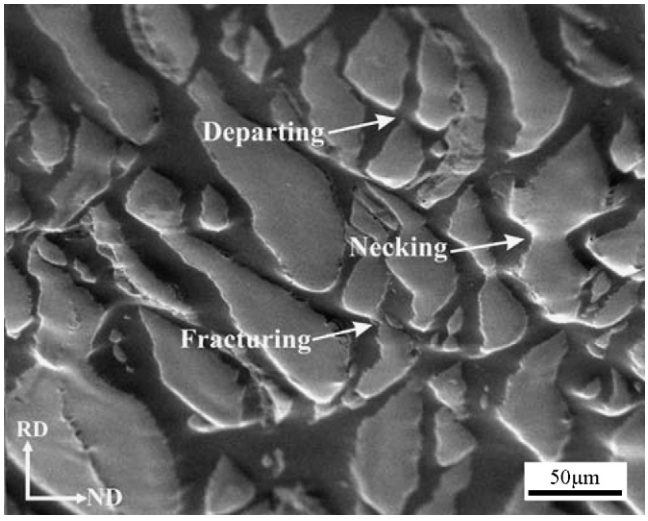

Fig. 2. SEM image of Al/Ni multilayer composite cross-section after the fourth cycle of ARB.

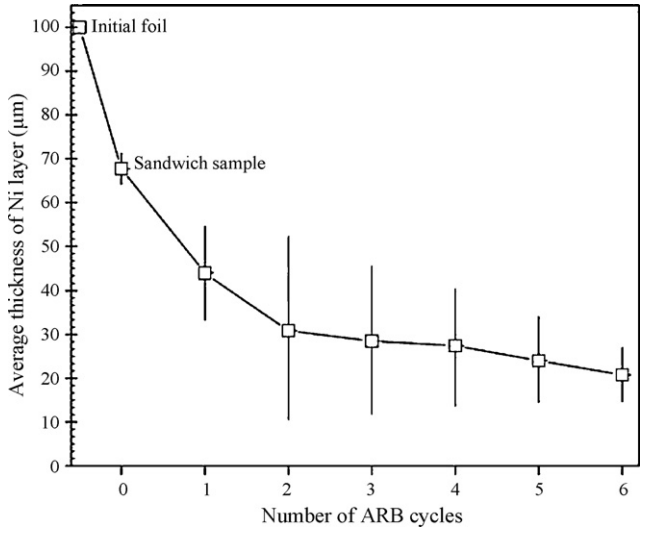

Fig. 3. Thickness variations of the nickel layers during different cycles of ARB of Al/Ni multilayer composite.

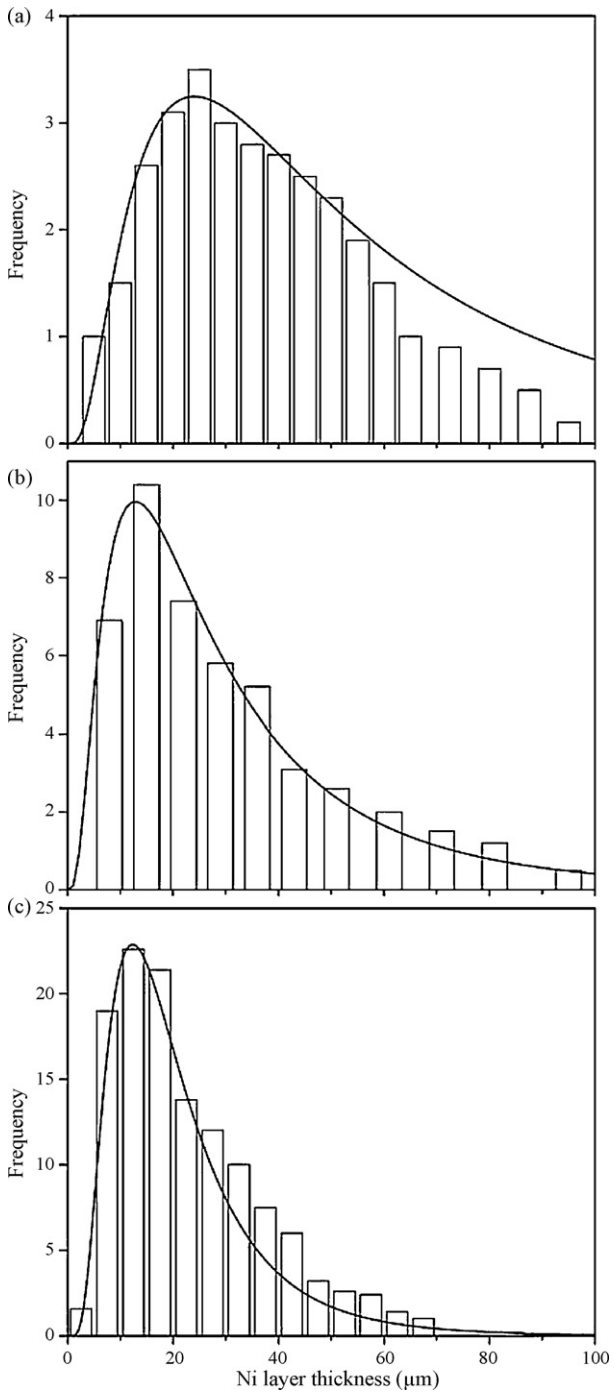

Fig. 4. Thickness frequency distribution of the Ni layers in Al/Ni multilayer composite and log normal fitted line after (a) 2 cycles, (b) 4 cycles and (c) 6 cycles of ARB process.

faces. Moreover, grain structure in the Ni layers is heterogeneous. Fig. 5 shows the grain structure of a nickel fragment at the edge and center zone. It was found that the grains are elongated at the edge of Ni layers, whereas equiaxed grains were formed in the center of these layers as in Fig. 5d. As mentioned above, large strain must have occurred at the two ends of Ni layers.

Physically, the softer matrix needs additional deformation to accommodate in the vicinity of harder Ni layers. Thus, it is expected that strain in the Al layers is more than the Ni layers due to the difference between the strength and work hardening exponent of them ($n_{Ni} = 0.387$ and $n_{Al} = 0.221$). Fig. 6 shows that the strain generated in Ni and Al layers in the initial stage of strain is approximately equal and close to the ideal isostrain condition, but with increasing the ARB cycles, strain in the Al layer become larger than that of which in the Ni layers. At early stage, nickel layers work harden quickly due to the higher work hardening exponent, and its strength increases more remarkably in comparison with Al layers. This process leads to strain accumulation in the Al layers and Al layers become thinner than the Ni fragments (Figs. 1 and 2).

The imposed plastic strains are not distributed equally for the Ni layers and Al matrix, and strain partitioning through thickness is also heterogeneous. It is reported that the relatively larger shear strain is introduced in surface regions in each ARB cycle due to the friction between the rolls and sample surfaces, which results in the change of grain size and different work hardening effects [21,30]. Moreover, heterogeneous strain distribution occurs in Ni layers and Al matrix due to the friction between the two metals caused by differences between flow properties.

Fig. 7a and b displays the composition profile across the Al/Ni interface after one and six cycles of ARB processes, respectively. These were obtained by EDX line scan analysis of a 4 μm line perpendicular to the Al/Ni interface. The EDX line scan along the interface of Ni and Al layers in the Ni/Al multilayer composite shows the diffusion of the two elements at the interface with increasing the cycles of ARB (Fig. 7b). Some local intermixing occurred at the interface of layers at higher cycles of ARB process and resulted in homogenous bonding. This phenomenon is known as a deformation induced interdiffusion process [11,18], which has also been observed during mechanical alloying process [31]. It consists of three basic mechanisms; mechanically induced atomic displacements, pipe diffusion along dislocations and severe plastic deformation induced vacancies [11,31]. The X-ray diffraction pattern from a cross-section of Al/Ni multilayer composite produced by six cycles of ARB (Fig. 8) shows that only aluminum and nickel phases are present at the interface of this composite. Therefore, no other products were formed at the interface, and since the binary phase diagram of Al/Ni shows no solid solution [23,29], the diffusion slope in Fig. 7b shows a nonequilibrium solid solution. This is not an equilibrium process because the EDX analysis shows some regions with a composition close to $Al_{50}Ni_{50}$ (Fig. 7). This corresponds to the composition of the ordered B2 NiAl phase. However, the XRD result did not show any intermetallic compound (Fig. 8).

3.2. Mechanical properties

The mechanical properties of primary sandwich and Al/Ni multilayer composites are summarized in Fig. 9. With regards to this figure, the yield strength and tensile strength of the Al/Ni composite increase with increasing the ARB cycles compared to the primary sandwich. The maximum yield strength and tensile strength reached 302 and 370 MPa respectively after 6 cycles. Uniform and total elongations decreased in the first two cycles, and then increased by increasing number of ARB cycles.

It has been stated that strength variations in severely deformed composites are governed by the two main strengthening mechanisms; strain hardening by dislocations and grain refinement [3,4,21,32–34]. In the early stages of ARB process, which a higher work hardening rate is imposed, the strength increases in cycles 1 and 2 due to work hardening [33,34]. After cycle 2, higher strength is achieved by grain refinement as the ARB cycles increase. As the effect of work hardening decreases, gradual evolution of ultrafine grains plays the main role in the strengthening. This effect is related to the increasing number of ultrafine grains and largely misoriented grain boundaries [4,32,35]. In the present work, strengthening of composites is not only resulted from the mentioned mechanisms, but it is also affected by the reinforcing role of the Ni layers in the Al matrix (Fig. 9) [2,21].

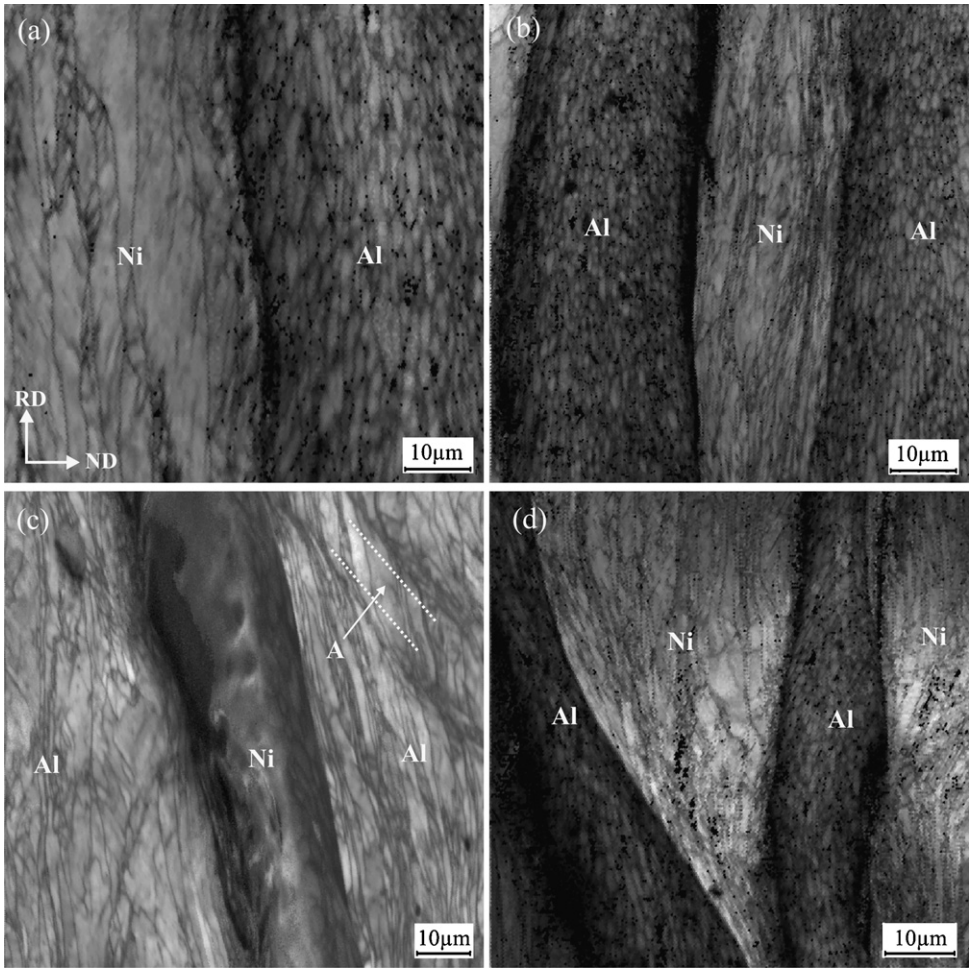

Fig. 5. SEM micrographs of electro etched cross-section of multilayer composite, (a) after 2 cycles, (b) 3 cycles, (c) 5 cycles and (d) 6 cycles of ARB process.

The engineering tensile strength and the total elongation of several materials are compared in Fig. 10—Al/Ni composite after 6 cycles (equivalent strain 5.3), aluminum 1060 foil (cold rolled with thickness of 100 μm), pure nickel foil (cold rolled with thickness of 100 μm), ARB processed Al/Al strip after 6 cycles (equivalent strain of 4.8) [3] and ARB processed Al/Cu multilayered composite after 5 cycles (equivalent strain of 4.6) [2]. With attention to this figure, the strength of both ARB processed Al/Al and Al/Ni multilayer com-

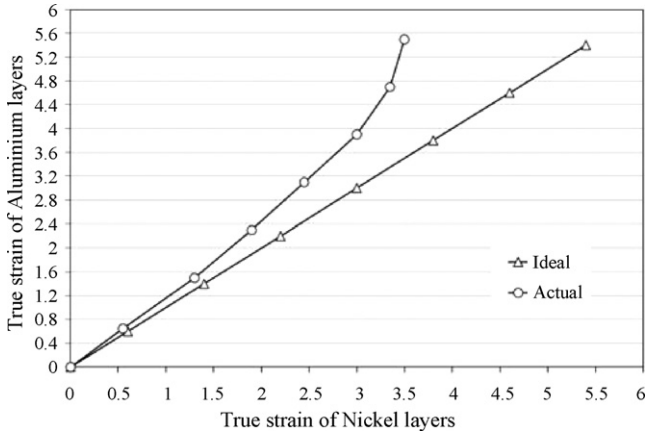

Fig. 6. Variation of true strain of Al and Ni layers with respect to ideal form, which define on isostrain condition for Al and Ni layers.

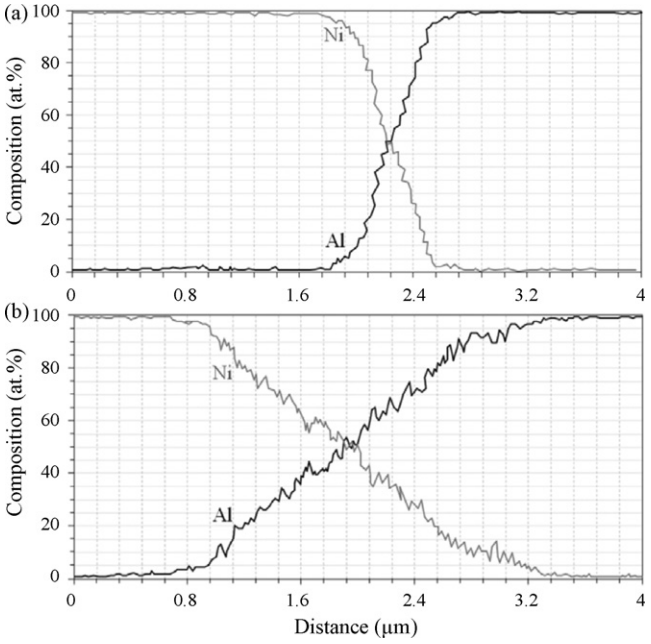

Fig. 7. EDX line scan at the interface of aluminum and nickel layers after (a) 1 cycle and (b) 6 cycles of ARB process.

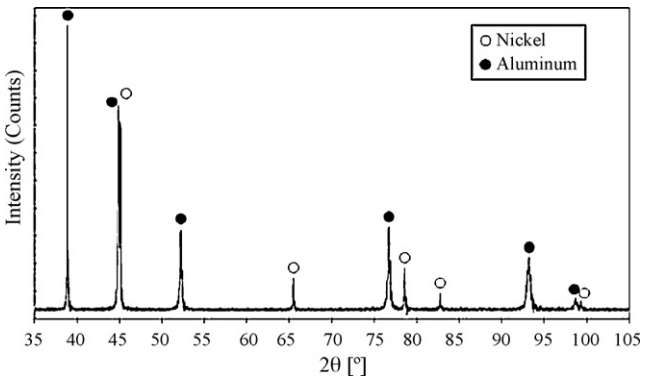

Fig. 8. XRD pattern from the cross-section of Al/Ni multilayer composite after 6 cycles of ARB process.

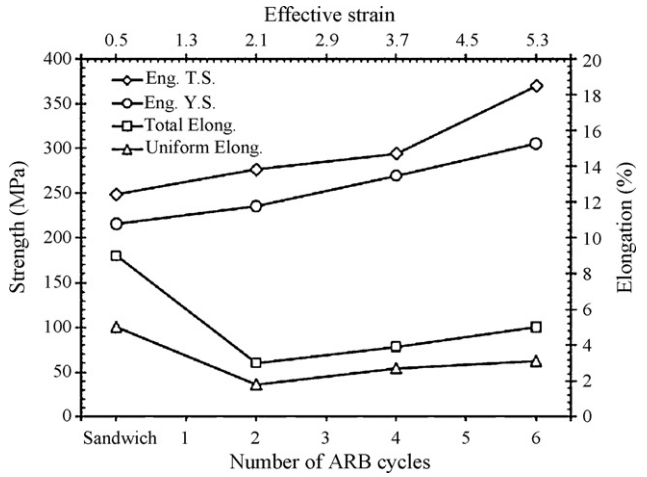

Fig. 9. Variation of strength and elongation of Al/Ni multilayer composite with respect to the number of ARB cycles.

posites increased in comparison to the commercial pure nickel and aluminum foil, whereas their elongation decreased in comparison to pure Al and Ni foil. A comparison of ARB processed Al/Al [3], Al/Cu [2] and Al/Ni composite demonstrates a higher strength for the Al/Ni multilayer composite, while elongations of Al/Cu composite and Al/Al are greater than the Al/Ni multilayer composite.

Furthermore, like other ARB processed materials [3,4,33–35] elongation decreased in the first two cycles due to the reduction of dislocations mobility as well as the small number of the existing shear bands. With increasing the number of ARB cycles, elongation increased (Fig. 9) due to the increase of the bond strength between matrix and reinforcement, as well as the thinning of Ni layers and their more uniform distribution in the matrix. One other reason could be that with increasing the ARB cycles, harder nickel layers become discontinuous, and softer aluminium layers play the role of the composite matrix.

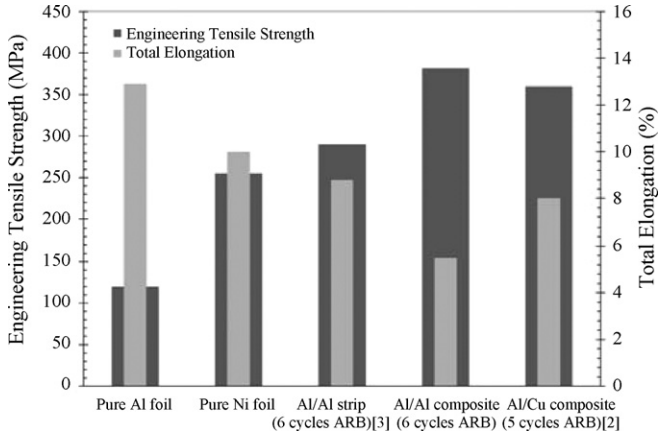

Fig. 10. Tensile strength and total elongation of commercial pure Al foil, pure Ni foil, ARB processed pure aluminum [3], Al/Ni and Al/Cu [2] multilayer composite.

Fig. 11 shows microhardness variations of aluminum and nickel layers at different cycles of ARB process. It illustrates that, as cycles increased, microhardness of both aluminum matrix and reinforcing nickel layers increased. Microhardness of both phases experienced a sharp rise in initial values from 27 and 81 to 86 and 141 VHN for aluminum and nickel layers respectively and followed by a moderate increase at intermediate cycles, and then, a plateau in the last cycles of the ARB process. It shows a high rate in the early cycles of ARB, and then, a lower rate for the last cycles. After the first and second cycles of ARB, the microhardness for aluminum matrix and nickel layers was approximately constant. In other words, work hardening for nickel layers and aluminum matrix is just is effective for the early cycles, and it does not contribute much in the later cycles of ARB process. Generally, hardening behavior in ARB processed ultrafine grained structures follows a trend which reaches stable condition. Rapid increase in microhardness for rather low strains was attributed mainly to the formation of subgrain boundaries and dislocations at the interface of Al and Ni layers, while grain refinement occurs in the later cycles [3,4,32]. Results show that the grain refinement contributed less in the increase of microhardness than in the work hardening mechanism [36].

As shown in Fig. 11, in early stage of ARB process there is a high difference between the maximum and minimum hardness in both aluminum and nickel layers. As ARB cycles increased, this difference decreased. It is because of the large amount of redundant shear strain introduced into the surface layers [30]. On continuing the ARB process, half of the surface layers come to the center in the next cycle, the repetition of this procedure causes more homogenous strain distribution through the composite thickness, leveling off the differences in hardness.

It is inferred that nickel layers influence the mechanical properties of the composites in two ways, direct and indirect [3,10]. For the direct mechanism, the layers bear part of the load exerted on the composites when the load is transferred from the matrix with shear action of the interface. For the indirect mechanism, the layers affect the microstructure of the composite in two aspects. On the

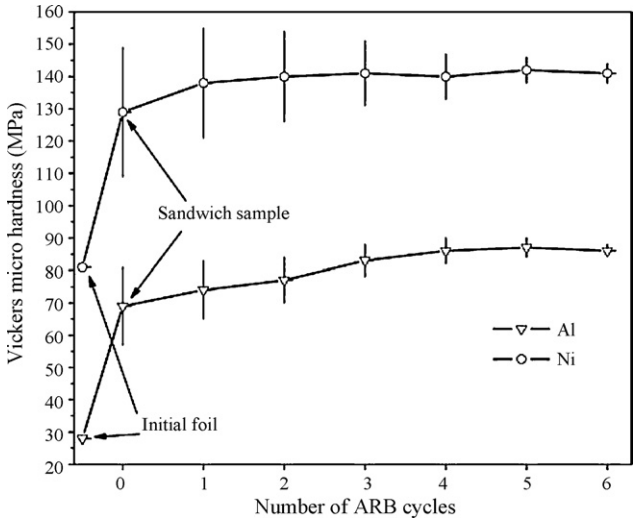

Fig. 11. Microhardness variation of nickel and aluminum layers of Al/Ni multilayer composite produced by ARB process.

one hand, the nickel reinforcements can refine the microstructure, and on the other hand, the tangling effects of dislocations around the nickel reinforcements may result in the increase of the strength and hardness.

4. Conclusion

Microstructural observation and mechanical measurements of ARB processed Al/Ni multilayer composites lead to the following conclusions:

(1) ARB process can be used to produce Al/Ni multilayer composites. With increasing the number of ARB cycles, nickel layers start to neck and fracture, leading to separation and fragmentation of this phase. After six cycles of ARB, a composite of aluminum matrix with uniform distribution of reinforcing phase (Ni) was obtained. Furthermore, nickel layers microstructure is not uniform. This is due to the non-uniform distribution of the strain originating from the friction between nickel and aluminum layers, as well as the shear strain gradient through the composite thickness.
(2) Strength and microhardness raised with increasing the number of ARB cycles, while elongation decreased with respect to the original values after the production of primary sandwich. Also, strength of the ARB processed Al/Ni multilayer composites is higher than the ARB processed pure aluminum in the same strain range due to the strengthening effect of reinforcing nickel fragments.
(3) Some nonthermodynamically intermixing occurred at the interface of the aluminum and nickel layers, but no intermetallic compound was formed.

References

[1] Y. Saito, H. Utsunomiya, N. Tsuji, T. Sakai, Acta Mater. 47 (1999) 579–583.
[2] M. Eizadjou, A. Kazemi Talachi, H. Danesh Manesh, H. Shakur Shahabi, K. Janghorban, Compos. Sci. Technol. 68 (2008) 2003–2009.
[3] M. Eizadjou, H. Danesh Manesh, K. Janghorban, J. Alloy Compd. 474 (2009) 406–415.
[4] N. Tsuji, Y. Ito, Y. Saito, Y. Minamino, Scripta Mater. 47 (2002) 893–899.
[5] H. Sieber, G. Wilde, J.H. Perepezko, J. Non-Cryst Solids 250–252 (1999) 611–615.
[6] N. Tsuji, T. Iwata, M. Sato, S. Fujimoto, Y. Minamino, J. Sci. Technol. Adv. Mater. 5 (2004) 173–180.
[7] S. Ohsaki, S. Kato, N. Tsuji, T. Ohkubo, K. Hono, Acta Mater. 55 (2007) 2885–2895.
[8] P.J. Hsieh, Y.P. Hung, J.C. Huang, Scripta Mater. 49 (2003) 173–178.
[9] R. Saha, R.K. Ray, D. Bhattacharjee, Scripta Mater. 57 (2007) 257–260.
[10] B.A. Movchan, F.D. Lemkey, Mater. Sci. Eng. A 224 (1997) 136–145.
[11] X. Sauvage, G.P. Dinda, G. Wilde, Scripta Mater. 56 (2007) 181–184.
[12] G. Min, J.M. Lee, S.B. Kang, H.W. Kim, Mater. Lett. 60 (2006) 3255–3259.
[13] H. Danesh Manesh, A. Karimi Taheri, J. Alloy Compd. 361 (2003) 38–143.
[14] R. Zhang, V.L. Acoff, Mater. Sci. Eng. A 463 (2007) 67–73.
[15] G.P. Dinda, H. Rösner, G. Wilde, Scripta Mater. 52 (2005) 577–582.
[16] H. Inoue, M. Ishio, T. Takasugi, Acta Mater. 51 (2003) 6373–6383.
[17] H.S. Ding, J.M. Lee, B.R. Lee, S.B. Kang, T.H. Nam, Mater. Sci. Eng. A 408 (2005) 182–189.
[18] R.J. Hebert, J.H. Perepezko, Scripta Mater. 50 (2004) 807–812.
[19] S.C. Jha, R.G. Delagi, J.A. Forster, P.D. Krotz, Metall. Mater. Trans. A 24 (1993) 15–20.
[20] K. Yasuna, M. Terauchi, A. Otsuki, K.N. Ishihara, P.H. Shingu, Mater. Sci. Eng. A 285 (2000) 412–417.
[21] M.C. Chen, H.C. Hsieh, W. Wu, J. Alloy Compd. 416 (2006) 169–172.
[22] P. Bhatt, V. Ganeshan, V.R. Reddy, S.M. Chaudhari, Appl. Surf. Sci. 253 (2006) 2572–2580.
[23] M. Holtz, D. Aurongzeb, M. Daugherty, A. Chandolu, J. Yun, J.M. Berg, H. Temkin, Mater. Res. Soc. Symp. Proc. 800 (2004) 4.7.1–4.7.6.
[24] T. Schmidt, H. Hoffmann, J. Magn. Magn. Mater. 248 (2002) 181–189.
[25] P.H. Shingu, K.N. Ishihara, A. Otsuki, I. Daigo, Mater. Sci. Eng. A 304–306 (2001) 399–402.
[26] A. Sagel, H. Sieber, H.J. Fecht, J.H. Perepezko, Acta Mater. 46 (1998) 4233–4241.
[27] J.M. Lee, B.R. Lee, S.B. Kang, Mater. Sci. Eng. A 406 (2005) 95–101.
[28] P. Bhattacharya, S. Bysakh, K.N. Ishihara, K. Chattopadhyay, Scripta Mater. 44 (2001) 1831–1835.
[29] H. Sieber, J.S. park, J. Weissmuller, J.H. Perepezko, Acta Mater. 49 (2001) 1139–1151.
[30] S.H. Lee, Y. Saito, N. Tsuji, H. Utsunomiya, T. Sakai, Scripta Mater. 46 (2002) 281–285.
[31] C.Y. Chunga, M. Zhub, C.H. Mana, Intermetallics 10 (2002) 865–871.
[32] Y. Saito, N. Tsuji, H. Utsunomiya, T. Sakai, R.G. Hong, Scripta Mater. 39 (1998) 1221–1227.
[33] Y.M. Wang, E. Ma, Acta Mater. 52 (2004) 1699–1709.
[34] N. Hansen, X. Huang, R. Ueji, N. Tsuji, Mater. Sci. Eng. A 387–389 (2004) 191–194.
[35] D. Terada, S. Inoue, N. Tsuji, J. Mater. Sci. 42 (2007) 1673–1681.
[36] Z.P. Xing, S.P. Kang, H.W. Kim, Scripta Mater. 45 (2001) 597–604.